Available online at www.sciencedirect.com
SCIENCE DIRECT®
Precambrian Research 124 (2003) 1–20
Precambrian Research
www.elsevier.com/locate/precamres

Typology and single grain U/Pb ages of detrital zircons from Proterozoic sandstones in the SW Urals (Russia): early time marks at the eastern margin of Baltica

A.P. Willner [a,*], S. Sindern [b,c], R. Metzger [b,c], T. Ermolaeva [b], U. Kramm [b], V. Puchkov [d], A. Kronz [e]

[a] *Institut für Geologie, Mineralogie und Geophysik, Ruhr-Universität, D-44795 Bochum, Germany*
[b] *Institut für Mineralogie und Lagerstättenlehre, RWTH, Wüllnerstr. 2, D-52056 Aachen, Germany*
[c] *Zentrallaboratorium für Geochronologie, Corrensstraße 24, D-48149 Münster, Germany*
[d] *Ufimian Geoscience Centre, Russian Academy of Science, K. Marx Street 16/2, 450000 Ufa, Russia*
[e] *Institut für Geochemie, Goldschmidtstr. 1, D-37077 Göttingen, Germany*

Received 13 November 2001; accepted 18 January 2003

Abstract

In the SW Urals a change of tectonic conditions occurred at around 620 Ma leading to a detrital input from contrasting provenance areas. Fifty-seven detrital zircons were separated from Proterozoic sandstones of this setting to study their typologies and pattern of U–Pb systematics.

Detritus from Riphean sandstones (1.63–0.65 Ga) contains three populations of zircon: (1) completely rounded fragmental grains with complicated, but weak internal fabrics derived from high grade metamorphic areas with multistage reworking; (2) long-prismatic zircon grains with rounded edges and weakly preserved growth zoning from S-type granites; (3) types 1 and 2, but cloudy due to intense alteration (hydration of metamict areas). Zircons from Upper Vendian sandstones (0.62–0.54 Ga) comprise two groups: (1) zircons similar to those of Riphean populations 1, 2 and 3; (2) perfectly euhedral zircons with preserved magmatic growth zoning from potassic alkaline as well as acid magmas.

Age signatures of polycyclic zircons from both Riphean and Upper Vendian detritus are compatible with crystallization in the interval of 1.8–2.3 Ga. This appears to be the significant age signature for the largely covered basement of the East European Platform, the presumed source region in the W. The pattern of U–Pb systems shows evidence of at least two events leading to lead loss. Data clusters in the concordia diagram confined to single samples show a remarkably strong influence of local sources. Alteration during diagenesis was an important factor of lead loss.

Upper Vendian detrital zircons have two sources: (1) The majority of the polycyclic rounded zircons also has a Paleoproterozoic crystallization age consistent with that of the Riphean detrital zircons. However, a few zircon grains point to a later anorogenic event which does not match with known events in the Riphean basin and hence underline an allochthonous character of the source area. (2) The data of the euhedral zircon would reflect a source age between 643 and 512 Ma.

The latter age signature is compatible with a local magmatic event concomitant with exhumation and emplacement of the allochthonous Beloretzk Terrane after 620 Ma. This eastern source area for the Upper Vendian detritus had partly been affected by high-pressure/low temperature metamorphism. The change of tectonic conditions reflected by the detritus composition

* Corresponding author. Fax: +49-234-32-14433.
E-mail address: arne.willner@ruhr-uni-bochum.de (A.P. Willner).

0301-9268/03/$ – see front matter
doi:10.1016/S0301-9268(03)00045-7

represents a change from a passive continental margin along the Rodinia supercontinent persisting during the Riphean to a convergent continental margin during the Upper Vendian within a transpressional setting.

Keywords: Zircon typology; Detrital zircon; Single grain U/Pb systematics; Timanide orogeny; Riphean sandstone; Vendian sandstone; Rodinia; SW-Urals

1. Introduction

During the past decade U–Pb-dating of single zircon crystals from all rock types combined with better imaging of their internal structures has provided a foundation to better understand many processes in general. Here we try to apply this combination of methods to detrital zircon crystals from the relatively well known Precambrian sedimentary basins in the Southern Urals.

The Urals represent a Variscan collisional orogen between the Baltica, Kazakhstanian and Siberian protocontinents with an intervening magmatic arc. At the eastern margin of Baltica a remarkably long Precambrian history of this margin can be detected below its Paleozoic cover (Fig. 1; Puchkov, 1997; Maslov et al., 1997). This early evolution is especially important in the light of recent efforts in understanding the formation and break up of the Late Precambrian supercontinent of Rodinia (e.g. Torsvik et al., 1996; Weil et al., 1998). The record is found in siliciclastic sediments from two contrasting, long persisting basins (Riphean and Vendian) between about 1.63 and 0.54 Ga. This period of time covers the entire history of assembly and dispersal of the Rodinia supercontinent.

The provenance signal of the detritus changes at around 620 Ma, which is consistent with the pre-Uralian Timanide orogeny (Puchkov, 1997; Maslov et al., 1997) representing a transition from a passive to an active continental margin (Willner et al., 2001). A similar history during the Neoproterozoic is observed, at least partly, along the entire length of the Urals on the western side of the suture zone, but it is definitely missing on the eastern (Siberian) side (Maslov et al., 1997; Puchkov, 1997).

Applying typological characterization and U–Pb systematics of single detrital zircon from siliciclastic rocks of the two different sedimentary piles with contrasting provenance areas, we attempt to answer the following methodological and regional issues:

- Does a systematic correlation exist between the internal structure and U–Pb isotope signature of the investigated zircon crystals?
- How does the internal structure and isotope information of the zircon crystals differ between the two contrasting types of detritus and how does this reflect different geological histories in the source areas?
- Is lead loss also caused by the process of diagenesis? Can we distinguish between isotope information of the source area and isotope disturbances from diagenetic processes ?
- Is the U–Pb isotope signature of the zircon crystals indicative for a specific protocontinent source?

From the stratigraphic sequence six zircon-rich samples of medium-grained non-metamorphosed sandstones were selected, four Riphean samples (8c, 32, 37, 40) and two Upper Vendian samples (18/19, 29). A thorough light and heavy mineral study of those samples has been performed previously (Willner et al., 2001).

2. Geological setting and evolution

The geological evolution at the eastern margin of Baltica starts within a Paleoproterozoic crystalline basement underlying the East European platform. Age information from these rocks, which are exposed e.g. in the Taratash Complex of the SW Urals (Fig. 1), was compiled by Lennykh and Krasnobaev (1978), Bogdanova (1986) and Ivanov et al. (1986). These data suggest a major Paleoproterozoic orogenic cycle between about 2.3 and 1.8 Ma based on U–Pb zircon data. This broad age pattern is confirmed by new data of Sindern et al. (2001) ranging between 2.34 and 1.8 Ga that can be correlated to specific geological processes. Granites (1.61–1.57; U–Pb) and diabase dykes (1.6 Ga; Rb–Sr) cutting the basement

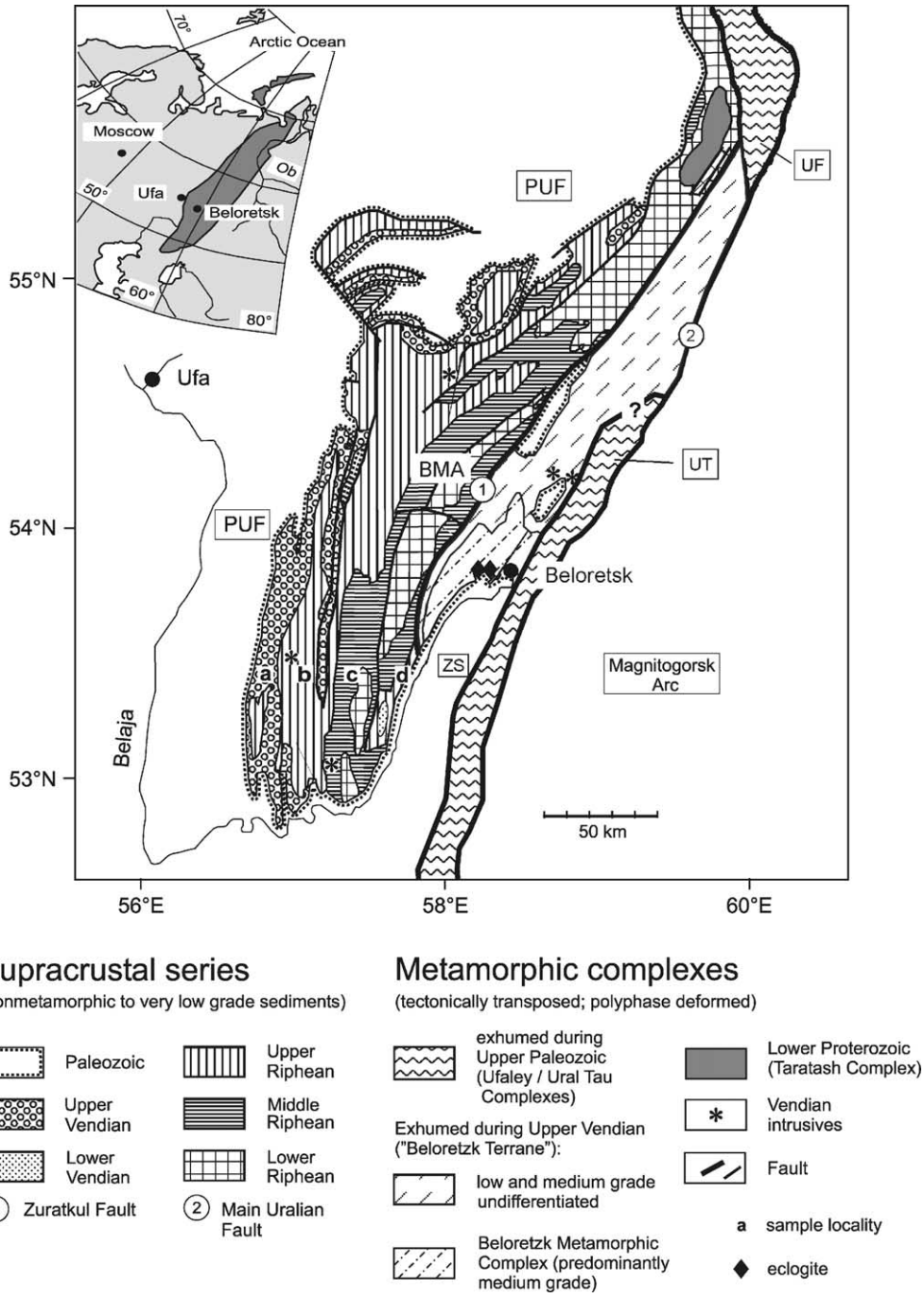

Fig. 1. Geological sketch map of the southwestern Urals. PUF Pre-Uralian Foredeep; BMA Bashkirian Megaanticlinorium; ZS Zilair Syncline; UT Ural Tau Antiform; BMC Metamorphic Complex of Beloretsk; UF Ufaley Metamorphic Complex. Samples studied for this paper were taken from the following localities: (a) 18/19, 22, 23, 28, 29; (b) 32; (c) 40; (d) 8c.

in the Taratash Complex are interpreted to be related to a younger rift event (Keller and Krasnobaev, 1983).

In the SW-Urals the overlying unmetamorphosed Proterozoic sediments are exposed in the Bashkirian Megaanticlinorium (Fig. 1). The 12–15 km thick, mainly siliciclastic sequence of the Riphean basin is subdivided by extrusions and intrusions of bimodal igneous rocks, which are related to three major rift events providing rough time markers around 1.65, 1.35 and 1.0 Ga (see Krasnobaev, 1986 and Maslov et al., 1997; Fig. 2). These ages are based on combined U/Pb dating on zircons and Rb/Sr whole rock isochrons. Sedimentation was partially under terrestrial conditions grading into shallow marine deposits towards the east (Maslov et al., 1997). The detrital components of the Riphean sandstones are characterized by a "continental platform provenance" in accordance to its derivation from the basement of the East European Platform (Willner et al., 2001). Supposed source rocks were granitoids and high grade metamorphic rocks as well as siliciclastic sediments and acid volcanic rocks reworked within the basin during episodic block faulting. The limited heavy mineral spectrum (zircon, tourmaline, rutile) provides evidence for polycyclic sedimentation.

The Riphean sediments are conformably overlain by Vendian siliciclastic sediments with a thickness of 2000–3000 m. While Lower Vendian sediments include glacial deposits, the Upper Vendian detritus was discharged from a proximal high-relief area in the east (Maslov et al., 1997; Willner et al., 2001) and deposited within a foredeep basin on the western flank of a pre-Uralian orogen (Puchkov, 1997) comprising mainly turbiditic sandstones and siltstones. Absolute ages of sedimentation of the Vendian siliciclastic rocks were mainly estimated from K/Ar and Rb/Sr-data from glauconites (see review of Maslov et al., 1997).

The provenance signal of the Upper Vendian sediments indicates a drastic change of tectonic conditions around 620 Ma (Willner et al., 2001). It has a "recycled orogenic provenance" including mineral and lithic clasts of mainly low grade siliciclastic metasediments and mylonites containing phengites with a high pressure signature as well as clasts of bimodal volcanic rocks and siliciclastic sediments derived from intrabasinal reworking. The heavy mineral spectrum is dominated by epidote, while the rest is rather reduced (zircon, tourmaline, rutile, apatite) suggesting polycyclic sedimentation and similarity to the Riphean heavy mineral spectrum.

The source area for the Upper Vendian detritus is still preserved between the Zuratkul Fault in the west and the Main Uralian Fault in the east (Fig. 1). This Beloretsk Terrane is characterized by low to medium grade metamorphic rocks, the latter dominating in its southern part (Metamorphic Complex of Beloretsk; Glasmacher et al., 1999, 2001; Fig. 1). Local lenses of eclogite occur within this complex. The country rocks contain phengite, which also implies high pressure during crystallization. White mica Ar–Ar cooling ages between 543 and 597 Ma (Glasmacher et al., 1999, 2001) suggest concomitant exhumation, surface uplift and emplacement of this complex during Vendian. A local granite gneiss has a protolith age of 950 Ma (zircon; Pb–Pb evaporation method; Glasmacher et al., 2001). In contrast to the interpretation of Glasmacher et al. (2001), we consider that this gneiss was deformed and metamorphosed along with the nearby eclogites between 950 and 718 Ma. The latter lower age limit of metamorphism is given by an Ar–Ar age of amphibole (Glasmacher et al., 2001). At that time there was ongoing sedimentation within the Bashkirian basin indicating an allochthonous derivation of the Beloretsk Terrane. Neoproterozoic deformation in Riphean sediments west of the Zuratkul fault is limited to weak folding, which decreases further west.

Small plutons, dykes and (sub)volcanic equivalents of a partly alkaline suite (alkali gabbro, essexite, syenite, monzonite, granite, rhyolite) represent a Vendian magmatic event according to Alekseev and Alekseeva (1980), because they cut Riphean, but not Upper Vendian sediments and have K–Ar ages between 602 and 670 Ma. Ar–Ar ages of 590–630 Ma for detrital orthoclase in the Upper Vendian given by Glasmacher et al. (1999) may also be attributed to cooling immediately following this magmatic event.

Ordovician sediments overlie the pre-Uralian basement east of the Zuratkul Fault and the Riphean basin further west with a pronounced angular unconformity (Puchkov, 1997). Later the entire area was incorporated into a westverging foreland fold-and-thrust belt during the Uralian orogeny.

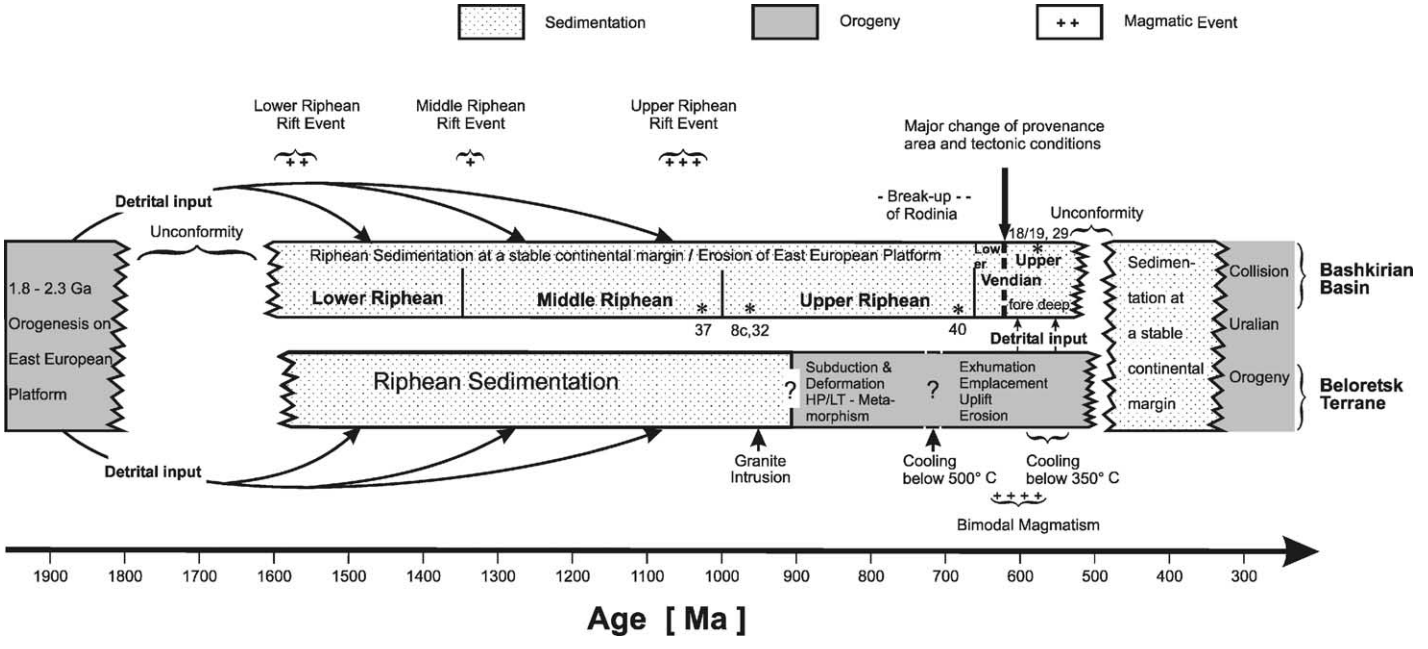

Fig. 2. Summary of Precambrian geological events in the SW Urals compatible with the results of this paper; the lithostratigraphic subdivision of Maslov et al. (1997) with the approximate stratigraphic position of the analysed samples (asterisk) is included.

3. Analytical methods

3.1. Sample selection and qualitative image analysis

Zircon crystals from Riphean and Vendian sandstones were selected from the spectrum of heavy minerals by magnetic separation and panning after dissolving of Fe stainings from the heavy minerals using 5N HCl during 5 min in an ultrasonic bath. A final selection and separation into colour, shape and transparency fractions was performed by hand-picking under the binocular microscope.

After a prior comprehensive study of light and heavy minerals in the Riphean and Vendian detritus (Willner et al., 2001) zircon crystals (grain size fraction 63–125 μm) were separated from those samples which show a typologically variable zircon population. Morphological studies on these populations were performed with a Zeiss scanning electron microscope at Aachen University. The typological classification scheme of Pupin (1980) was used.

Ninety two selected grains were embedded in epoxy resin, mostly cut parallel to {1 0 0} prism zones and polished. Backscattered electron images, cathodoluminescence images, element distribution maps and qualitative energy-dispersive analysis of inclusions and alteration zones were performed with a Jeol JXA 8900 RL microprobe at Göttingen University and a Cameca SX 50 microprobe at Bochum University. A complete set of images can be obtained upon request from the senior author.

3.2. Zircon preparation for isotope analysis

Fifty to hundred transparent, colourless and inclusion free crystals per zircon fraction were cleaned in H_2O, heated for 30 min at 80 °C and washed finally four times with acetone. All reagents were of ultrapure grade.

The marginal shells of part of the selected crystals were partly abraded in a mill as described by KROGH (1982) using pyrite as an abrasive. These zircon crystals were cleaned from adhesive pyrite by washing with 7.5N HNO_3 for 30 min at 50 °C and rinsing with H_2O and acetone. The weight of the single zircons was not determined because of their size, hence, the concentrations of Pb and U cannot be calculated from the isotopic data.

Digestion of original and abraded zircon crystals was performed in teflon liners designed for the dissolution of six single crystals simultaneously using 24N HF at 180 °C (vapour digestion technique according to Wendt, 1993). The digestion was completed after 4 days. After spiking with a mixed ^{205}Pb–^{233}U solution sample and spike were homogenized in 6N HCl for 24 h at 80 °C. The excess HCl was evaporated finally.

3.3. Mass spectrometry

The Pb standards as well as the spiked samples were loaded without element separation on single Re filaments (Wendt, 1993) into a silica gel bed with 2 μl of a loading solution containing 90 vol.% of 6N HCl and 10 vol.% of 0.1N H_3PO_4.

Isotope measurements were performed on a VG sector 54 mass spectrometer at the Zentrallabor für Geochronologie, Münster University, equipped with a Daly multiplier. The Pb composition was determined at 1300–1400 °C followed by the U measurement at 1400–1450 °C. At maximum the $2\sigma_m$ errors obtained for $^{206}Pb/^{204}Pb$, $^{207}Pb/^{206}Pb$, and $^{233}U/^{238}U$ were 3.0, 0.05, and 0.1%, respectively (see Table 1 for individual absolute errors). The isotope ^{208}Pb was not analysed. Isotope ratios were corrected for mass fractionation (0.11% ± 0.02/amu), blank (<10 pg total Pb, $^{206}Pb/^{204}Pb = 17.7 \pm 0.5$, $^{207}Pb/^{204}Pb = 15.5 \pm 0.1$, 1 pg U) and initial common Pb estimated after the model of Stacey and Kramers (1975). The $^{206}Pb/^{204}Pb$ and $^{207}Pb/^{204}Pb$ ratios were deduced from the latter model using the apparent $^{207}Pb/^{206}Pb$ ages. Uncertainties of the $^{206}Pb/^{204}Pb$ and $^{207}Pb/^{204}Pb$ ratios were assumed to be 2 and 0.3%, respectively. Decay constants are taken from Jaffey et al. (1971).

4. Typology of zircon

4.1. Detrital zircons from Riphean sandstones

Among zircon grains separated from four Riphean sandstones (8c, 32, 37, 40; see appendix for petrography) three groups can be distinguished based on morphology and type of internal zoning:

Table 1
Analytical data of the studied U–Pb systems

Sample	Zircon group	Pb[a] (pg)	U[b] (pg)	$^{206}Pb/^{204}Pb$ ratio[c] and $2\sigma_m$ error	$^{207}Pb/^{206}Pb$ ratio[d] and $2\sigma_m$ error	$^{207}Pb/^{235}U$ ratio[d] and $2\sigma_m$ error	$^{206}Pb/^{238}U$ ratio[d] and $2\sigma_m$ error	$^{207}Pb/^{206}Pb$ age (Ma)	$^{207}Pb/^{235}U$ age (Ma)	$^{206}Pb/^{238}U$ age (Ma)
Riphean										
40Z1-0	I	56	216	264.3 ± 0.2	0.09216 ± 0.00058	2.853 ± 0.027	0.2246 ± 0.0014	1471	1370	1306
40Z1-1	I	56	214	248.5 ± 0.2	0.09141 ± 0.00057	2.838 ± 0.029	0.2251 ± 0.0017	1455	1366	1309
40Z1-2	I	39	189	294.3 ± 0.3	0.09023 ± 0.00060	2.258 ± 0.023	0.1815 ± 0.0013	1430	1199	1075
40Z1-3	I	35	146	276.7 ± 0.3	0.09723 ± 0.00058	2.820 ± 0.027	0.2104 ± 0.0015	1572	1361	1231
40Z1-4	II	26	111	211.4 ± 0.2	0.09002 ± 0.00063	2.525 ± 0.027	0.2034 ± 0.0014	1426	1279	1194
40Z1-5	II	33	137	273.5 ± 0.1	0.08873 ± 0.00044	2.560 ± 0.019	0.2092 ± 0.0010	1398	1289	1225
32Z3r-0	I	22	68	104.9 ± 0.8	0.12760 ± 0.00179	4.307 ± 0.119	0.2448 ± 0.0056	2065	1695	1411
32Z3r-1	I	78	215	275.0 ± 0.2	0.12292 ± 0.00048	5.214 ± 0.036	0.3076 ± 0.0016	1999	1855	1729
32Z3r-2	I	92	259	331.3 ± 0.3	0.12639 ± 0.00073	5.264 ± 0.049	0.3021 ± 0.0021	2048	1863	1701
32Z3r-3	I	77	222	145.7 ± 0.5	0.12834 ± 0.00117	4.842 ± 0.058	0.2736 ± 0.0018	2075	1792	1559
32Z3r-5/1	I	44	121	175.9 ± 1.1	0.12327 ± 0.00245	4.995 ± 0.127	0.2939 ± 0.0041	2004	1818	1661
32Z3r-5/2	I	44	121	179.5 ± 0.9	0.12792 ± 0.00156	5.252 ± 0.081	0.2978 ± 0.0022	2070	1861	1680
32Z3r-0	I	94	240	693.5 ± 0.1	0.12186 ± 0.00040	5.763 ± 0.035	0.3430 ± 0.0017	1984	1941	1901[e]
32Z3-1	I	97	245	686.1 ± 0.3	0.12009 ± 0.00057	5.748 ± 0.040	0.3471 ± 0.0016	1958	1939	1921[e]
32Z3-2	I	98	245	562.1 ± 0.1	0.12171 ± 0.00034	5.814 ± 0.034	0.3465 ± 0.0017	1981	1949	1918[e]
32Z3-3	I	98	246	479.7 ± 0.2	0.12223 ± 0.00041	5.820 ± 0.035	0.3453 ± 0.0017	1989	1949	1912[e]
32Z3r-4	I	97	242	441.2 ± 0.2	0.12094 ± 0.00044	5.761 ± 0.039	0.3455 ± 0.0019	1970	1941	1913[e]
32Z3-5	I	95	239	506.9 ± 0.2	0.12075 ± 0.00039	5.729 ± 0.033	0.3441 ± 0.0016	1967	1936	1906[e]
8cZ1-0	II	108	336	1512.5 ± 0.1	0.11369 ± 0.00022	4.485 ± 0.019	0.2861 ± 0.0011	1859	1728	1622
8cZ1-1	II	61	257	987.3 ± 0.1	0.09475 ± 0.00027	2.814 ± 0.013	0.2154 ± 0.0008	1523	1359	1258
8cZ1-2	II	179	693	2062.0 ± 0.1	0.10681 ± 0.00019	3.418 ± 0.017	0.2321 ± 0.0011	1746	1509	1345
8cZ1-3	II	196	778	2524.0 ± 0.1	0.10866 ± 0.00018	3.385 ± 0.015	0.2260 ± 0.0009	1777	1501	1313
8cZ1-4	II	214	853	2881.6 ± 0.1	0.10665 ± 0.00019	3.329 ± 0.016	0.2264 ± 0.0010	1743	1488	1315
8cZ1-5	II	175	605	2496.7 ± 0.1	0.10898 ± 0.00017	3.906 ± 0.016	0.2600 ± 0.0010	1782	1615	1490
37bZ1-1	I	69	186	681.8 ± 0.3	0.13667 ± 0.00050	6.067 ± 0.044	0.3220 ± 0.0019	2185	1986	1799
37bZ1-2	I	33	85	380.5 ± 0.9	0.13198 ± 0.00138	6.078 ± 0.083	0.3340 ± 0.0022	2124	1987	1858

Table 1 (*Continued*)

Sample	Zircon group	Pb[a] (pg)	U[b] (pg)	$^{206}Pb/^{204}Pb$ ratio[c] and $2\sigma_m$ error	$^{207}Pb/^{206}Pb$ ratio[d] and $2\sigma_m$ error	$^{207}Pb/^{235}U$ ratio[d] and $2\sigma_m$ error	$^{206}Pb/^{238}U$ ratio[d] and $2\sigma_m$ error	$^{207}Pb/^{206}Pb$ age (Ma)	$^{207}Pb/^{235}U$ age (Ma)	$^{206}Pb/^{238}U$ age (Ma)
Upper vendian										
18/19Z3r-0	I	143	431	173.8 ± 0.2	0.11947 ± 0.00071	5.128 ± 0.045	0.3113 ± 0.0017	1948	1841	1747
18/19Z3r-1	I	140	375	206.6 ± 0.2	0.11826 ± 0.00058	5.027 ± 0.051	0.3083 ± 0.0026	1930	1824	1732
18/19Z3r-2	I	54	137	180.6 ± 0.1	0.11877 ± 0.00062	5.280 ± 0.044	0.3224 ± 0.0019	1938	1866	1802
18/19Z3r-3	I	71	169	129.3 ± 0.4	0.11918 ± 0.00106	5.358 ± 0.064	0.3261 ± 0.0022	1944	1878	1819
18/19Z3r-5	I	92	243	183.0 ± 0.2	0.11792 ± 0.00061	5.020 ± 0.049	0.3087 ± 0.0024	1925	1823	1734
18/19Z1r-0	I	79	223	1135.5 ± 0.1	0.11841 ± 0.00031	5.128 ± 0.030	0.3141 ± 0.0016	1932	1841	1761
18/19Z1r-1	I	42	160	586.1 ± 0.2	0.09276 ± 0.00123	3.018 ± 0.042	0.2360 ± 0.0010	1483	1412	1366
18/19Z1r-2	I	72	201	1152.6 ± 0.1	0.11293 ± 0.00053	4.974 ± 0.032	0.3195 ± 0.0014	1847	1815	1787
18/19Z1r-4	I	43	120	602.6 ± 0.1	0.10930 ± 0.00070	4.702 ± 0.037	0.3120 ± 0.0013	1788	1768	1750
18/19Z1r-5	I	19	68	331.1 ± 0.3	0.09061 ± 0.00059	3.108 ± 0.027	0.2488 ± 0.0012	1438	1435	1432
18/19Z3rb2	I	72	189	323.3 ± 0.2	0.11810 ± 0.00050	5.290 ± 0.040	0.3249 ± 0.0019	1928	1867	1814
18/19Zrb3	I	92	189	73.5 ± 1.7	0.12711 ± 0.00330	5.939 ± 0.183	0.3389 ± 0.0033	2058	1967	1881
18/19Zrb4	I	71	189	335.9 ± 0.2	0.11798 ± 0.00042	5.283 ± 0.033	0.3248 ± 0.0016	1926	1866	1813
18/19Z3ra0	I	72	190	291.3 ± 0.2	0.11814 ± 0.00051	5.283 ± 0.040	0.3244 ± 0.0019	1928	1866	1811
18/19Z3ra-1	I	74	189	239.2 ± 0.2	0.11863 ± 0.00050	5.336 ± 0.040	0.3263 ± 0.0018	1936	1875	1820
18/19Z3ra5	I	74	189	213.5 ± 0.1	0.11738 ± 0.00055	5.268 ± 0.039	0.3255 ± 0.0017	1917	1864	1817
18/19-Z4-0	IIa	14	462	132.4 ± 0.6	0.05902 ± 0.00132	0.898 ± 0.023	0.1103 ± 0.0010	568	650	675
18/19-Z4-1	IIa	14	354	113.0 ± 0.4	0.06109 ± 0.00118	0.916 ± 0.020	0.1087 ± 0.0006	643	660	665
18/19-Z4-4	IIa	15	181	98.2 ± 0.4	0.05917 ± 0.00130	0.824 ± 0.021	0.1010 ± 0.0007	573	610	620
18/19-Z4-5	IIa	15	505	134.8 ± 0.6	0.05815 ± 0.00125	0.874 ± 0.021	0.1090 ± 0.0006	535	638	667
18/19Z4-0	IIa	14	105	64.9 ± 0.7	0.06055 ± 0.00215	0.777 ± 0.031	0.0931 ± 0.0009	623	584	574
18/19Z4-1	IIa	15	104	60.5 ± 0.5	0.06044 ± 0.00203	0.776 ± 0.029	0.0931 ± 0.0008	619	583	574
18/19Z4-3	IIa	14	104	69.3 ± 0.3	0.05869 ± 0.00156	0.754 ± 0.023	0.0931 ± 0.0007	556	570	574
18/19Z4-4	IIa	15	104	53.0 ± 0.3	0.05754 ± 0.00209	0.743 ± 0.030	0.0936 ± 0.0008	512	564	577
18/19Z4-5	IIa	16	105	52.8 ± 1.0	0.06043 ± 0.00330	0.780 ± 0.047	0.0936 ± 0.0009	619	585	577
29Z1-1	I	96	226	103.7 ± 0.2	0.11725 ± 0.00094	5.180 ± 0.060	0.3204 ± 0.0023	1915	1849	1792
29Z1-4	I	87	227	183.2 ± 0.2	0.11736 ± 0.00066	5.074 ± 0.045	0.3136 ± 0.0019	1916	1832	1758
29Z1-5	I	93	228	123.8 ± 1.0	0.12104 ± 0.00195	5.271 ± 0.103	0.3158 ± 0.0024	1972	1864	1769
29Z10	I	85	229	234.8 ± 0.2	0.11615 ± 0.00051	4.962 ± 0.040	0.3098 ± 0.0019	1898	1813	1740
29Z12	I	84	226	244.3 ± 0.2	0.11737 ± 0.00059	5.022 ± 0.043	0.3103 ± 0.0020	1917	1823	1742
29Z13	I	85	228	213.8 ± 0.3	0.11716 ± 0.00064	5.027 ± 0.043	0.3112 ± 0.0018	1913	1824	1746

[a] Amount of ^{207}Pb, ^{206}Pb and ^{204}Pb in zircon.
[b] Atomic ratios corrected for blank, spike, fractionation and initial common Pb.
[c] Amount of U in zircon.
[d] Corrected for spike and fractionation.
[e] Further abraded.

Zircon *group I* (19 grains) comprises clear, colourless, generally perfectly rounded fragments of larger crystals (Fig. 3(1 and 2)) suggesting multistage reworking. The surfaces are mostly rough and pitted. The degree of fracturing and filling of fractures is variable. The type of internal zoning also varies considerably, but is always faint and cathodoluminescence is usually very weak. Some grains even appear unzoned in back scatter electron images. Apart from some former well-developed, concentric growth zonation partly with traces of round dissolution surfaces, relict zoning is generally hazy and diffuse (Fig. 3(1)). Also blurred former oscillatory zoning without distinct borders occurs. Internal unconformities due to overgrowth phenomena are frequent. Patchy zoning with sharp and curved sectoral boundaries, planar and non-planar sectoral overgrowth as well as some older inherited cores are observed. Two grains show fir-tree sector zoning in overgrowth rims (Fig. 3(2)) as described by Vavra et al. (1996). Tiny, round inclusions of apatite and quartz are abundant. In one grain inclusions of Cl-rich apatite were observed.

Group I internal fabrics are rather similar to zircon from amphibolite and granulite facies terranes as described by Vavra et al. (1996, 1999) and Schaltegger et al. (1999). The low contrasts between adjacent individual growth bands are inferred to be due to small chemical differences and may be interpreted as gradual erasing of primary zoning either by diffusion under elevated temperatures or by annealing effects within strained lattice domains as suggested by Schaltegger et al. (1999). Inherited zircon can occur as xenocrysts or detrital cores that are overgrown in a complex manner. Observed patchy, sector or fir-tree zones and thin overgrowths at the rims are due to subsolidus crystallisation.

Zircon *group II* (11 grains) comprises clear, colourless and long prismatic grains (S11, S12 and S17 type after Pupin, 1980) that are edge rounded to variable degrees (Fig. 3(3 and 4)). The crystals are partly broken at one end along fresh cracks. The surfaces are generally rough and pitted, but a few grains are euhedral with smooth surfaces. Filled cracks are always developed. Round inclusions of magnetite, Fe-rich biotite, K-feldspar, quartz, xenotime and apatite needles were observed.

A perfect concentric, narrowly spaced, oscillatory growth zoning pattern is generally developed. The grains can display cores with traces of round dissolution surfaces (Fig. 3(3)) and planar overgrowth. Three grains contain a round inherited core. Small filled dissolution embayments can also occur at the edges of the grains. Most grains show outer planar overgrowth zones at the edges.

Group II typically comprises magmatic zircon. Morphology, typical inclusions as well as some occurrence of inherited cores point to (at least partly S-type) granitoids as source rocks. Resorption during zircon growth can be due to the onset of anatexis or changing PTAX conditions in a magma (Vavra et al., 1996, 1999). Edge rounding points to less abrasive transport compared to group I zircon. The coincidence of features indicating less transport with specific zoning, morphology and inclusion types suggests a rather local and more restricted detritus information compared to the more variable group I zircon with longer transport.

Zircon *group III* (21 grains) includes groups I and II type grains characterised by alteration as a prominent additional feature (Fig. 3(5 and 6)). These grains are typically cloudy and coloured (brownish, yellowish or reddish).

Irregular patches of alteration (darker in BSE images than the surroundings and with spotted appearance) are bound to specific growth zones that can also be entirely affected. Alteration zones are mostly located near the edges of the zircon grains or can even affect the entire zircon except an outer overgrowth (Fig. 3(6)). Abundant prominent filled cracks propagate from the rims and end in alteration zones (Fig. 3(5)) or can be confined to individual growth zones being oriented perpendicular to growth surfaces and radial to the centre. In larger zones alteration forms irregular halos or fronts around crack terminations. Alteration starts along cracks that are widened and first affects specific narrow crystallographic zones. If the net of cracks becomes denser, more alteration occurs. In extreme cases alteration also affects previously unaltered zones changing finally the entire crystal with some remaining unaltered islands.

In BSE images two different types of alteration can be distinguished that can even occur within a single grain: dark zones being relatively enriched in Ca and Al compared to the unaltered zones, while slightly brighter zones are relatively enriched in Fe with few Ca and no Al. Relative enrichment of these elements as well as of Y and P prove alteration.

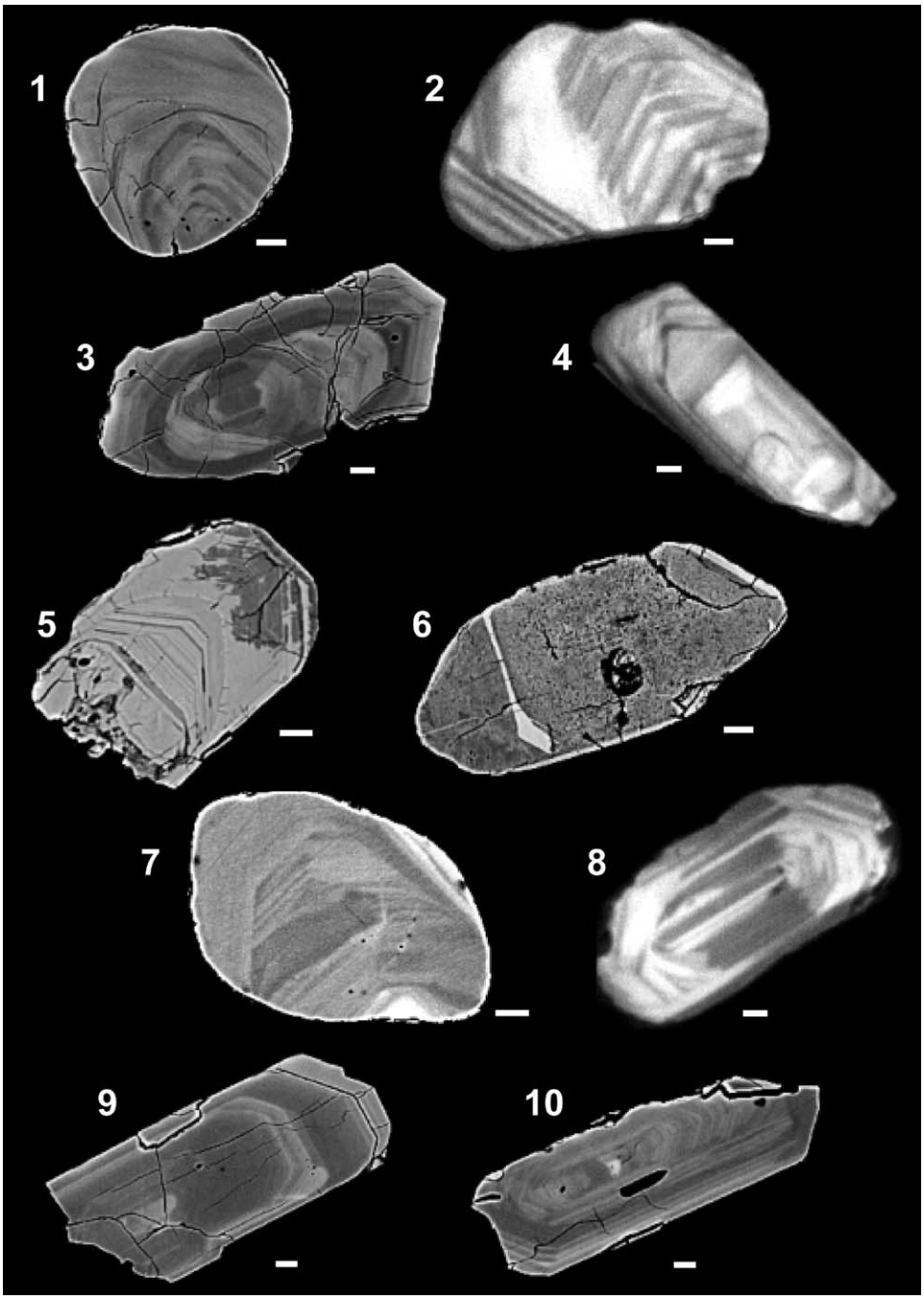

Fig. 3. Images of polished zircon crystals (for explanation see text): *Riphean zircon*: 1, 2 group I; 3, 4 group II; 5, 6 group III; *Vendian zircon*: 7 subgroup Ia; 8 subgroup Ib; 9 subgroup IIa; 10 subgroup IIb 1, 3 5, 6, 7, 9, 10 BSE images; 2, 4, 8 CL images; all scales are 10 μm.

Lee and Tromp (1995) pointed out that microcracks as potential fluid pathways for alteration can be induced by metamictisation. This process leads to lattice expansion due to high local radiation damage which also weakens certain zircon zones locally that can be preferably altered. Alteration is presumably an effect of hydration in metamict areas as was suggested by Medenbach (1976). Kurz (2000) altered zircon experimentally with hydrothermal Ca-rich fluids proving the observed effects and a considerable U and Pb mobility. Clear zircon became cloudy.

Yet it is not clear whether alteration happened in the source rock during a specific hydrothermal event or enclosed in the sandstone either due to continuous exposure to sedimentary brines or a more time-restricted hydrothermal event. However, if we regard the very long exposure of the Riphean zircon to formation water in the Bashkirian basin and also the fact that nearly all Riphean zircon show at least some effects of alteration, sedimentation and diagenesis are the most probable alteration processes.

4.2. Detrital zircons from Upper Vendian sandstones

Two major groups of zircon may be distinguished in the Vendian sandstones (see appendix for petrography), rounded recycled (Vendian group I) and fresh euhedral individuals (Vendian group II).

Group I contains rounded, i.e. recycled and older zircon grains that allow a further subdivision into three subtypes:

Subgroup Ia zircons (17 grains) are clear, partly colourless and partly coloured (yellowish, brownish), but well rounded with rough and pitted surfaces. Most are nearly ball-shaped, some slightly elongated, but always fragments of bigger original crystals. Zoning is generally diffuse, hazy or patchy, irregular rather than concentric, with extremely faint differences between the zones and mostly blurred transitions (Fig. 3(7)). Some faint relict concentric zoning may still be visible with catodoluminescence. Boundaries of patchy sectors are planar or curved. Four grains show fir-tree zoning. One grain contains a discordant core. Small non-planar concentric overgrowth at the rims occurs sometimes. The degree of filled cracks varies. Very small round inclusions dominate over rare larger inclusions of plagioclase, quartz, euhedral apatite as well as Fe- and Ti-rich biotite.

Subgroup Ib zircons (8 grains) consist of long-prismatic, but moderately rounded grains with rough and pitted surfaces. They seem to have a S-type morphology after Pupin (1980). They show faint former concentric magmatic growth zoning with rather narrowly spaced zones parallel to the prism planes (Fig. 3(8)). Sectoral zoning and discordant cores are rare as well as filled cracks. Sometimes slight planar and nonplanar overgrowth is observed at the rims. Tiny inclusions of quartz and K-feldspar are always round.

Five *subgroup Ic* grains are similar to those of Ib subtype, but are cut by abundant filled cracks terminating in narrow patchy alteration zones parallel to former growth zones. Strong alteration in the outermost zones is characteristic.

All group I subtypes show most features also observed in groups I-III of Riphean zircon. This includes similar S-type typologies, inclusion minerals and occurrence of inherited cores within long-prismatic edge-rounded varieties that point to granitoid source rocks of crustal origin as well as zoning pattern typical for zircon from high grade metamorphic areas. Alteration appears to be much less frequent.

Among the euhedral zircon grains (*group II*) two subtypes can be distinguished that derived from two different magmatic rocks as constrained by their morphology and their inclusion types:

Group IIa (12 grains) consists of perfectly euhedral, columnar grains that are clear, slightly yellowish-greenish and contain abundant inclusions. Surfaces are perfectly smooth. P-type zircon (P2, P3, P4; P5 after Pupin, 1980) dominates, more rarely S-type grains are found (S19, S24). All sections parallel {1 0 0} show perfect igneous concentric, strongly oscillatory and sometimes slight sectoral zoning (Fig. 3(9)). Round or concave traces of unconformably overgrown dissolution surfaces occur in some. Xenocryst cores were not observed. Incipient alteration in the outermost growth zone was only observed in two grains. Among very abundant inclusions are Ti- and Fe-rich biotite, K-feldspar, Cl-rich apatite, Mn-rich ilmenite and very small round monazite grains.

Zircon morphology and the type of inclusions point to Si-undersaturated potassic alkaline magmas such as

syenite as the most probable source. Pebbles of syenite are abundant in the immediately overlying Kukkarauk conglomerate. The perfect euhedral shape and the high concentration of group IIa zircons with respect to other Upper Vendian sandstones indicates a nearby local source for group IIa zircon grains as for the conglomerate pebbles.

Three further long-prismatic grains (*subgroup IIb*; Fig. 3(10)) show similar features (P2; P4 type), but contain quartz, magnetite, Mn-free ilmenite and K-feldspar as inclusions. Also incipient alteration in an outermost zone is observed in two zircon grains. This evidently less abundant group of zircon resembles zircon from a Si-saturated melt. Rhyolite that also occurs among pebbles in the conglomerate of the Upper Vendian Kukkarauk Formation is a possible source rock.

5. Geochronological results

For the U–Pb isotope determinations we tried to use clear and colourless zircon crystals only to avoid alteration as far as possible as an additional process modifying the U–Pb-systematics. Nevertheless, due to the random occurrence of this feature even at a small scale, no exclusive avoidance is possible.

5.1. Riphean samples

All U–Pb systems analysed in all samples are discordant (Figs. 4 and 5). Due to the low amount of radiogenic Pb in some analyses relatively large errors occur (Table 1). Surprisingly, the U–Pb-data of the Riphean samples show separation into four distinctly different clusters in the U–Pb-concordia diagram for

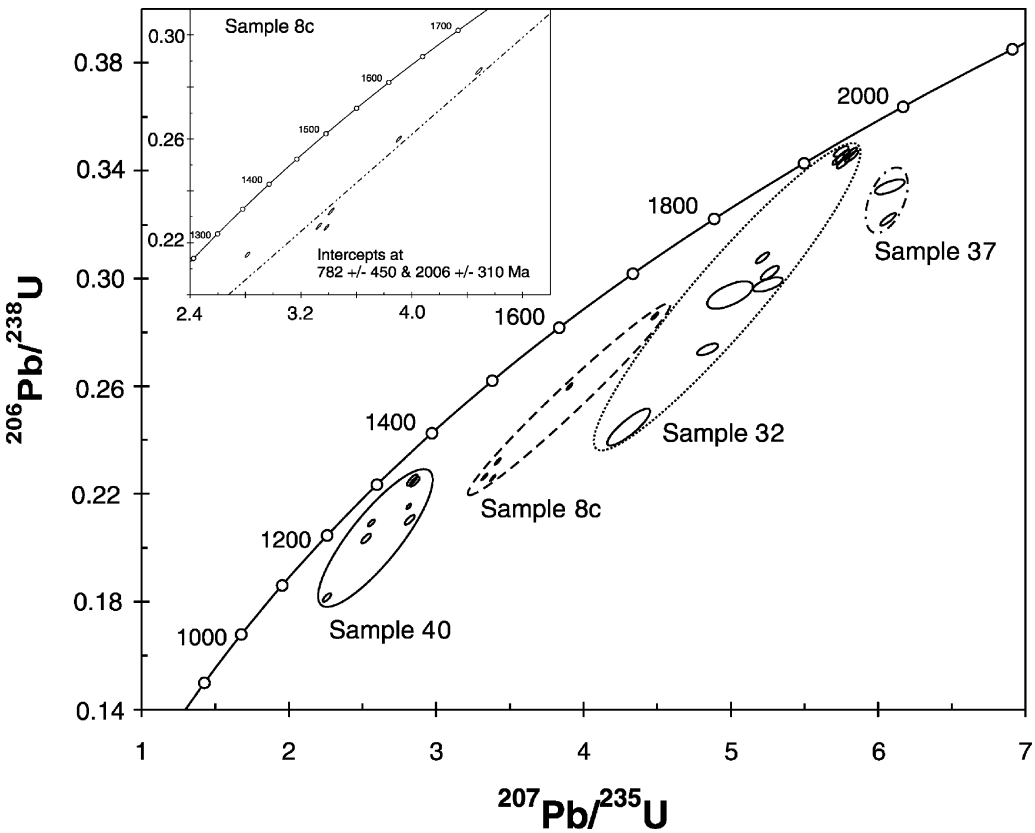

Fig. 4. Synoptic concordia diagram showing single grain U–Pb data of detrital zircons in all analysed Riphean samples (8c, 32, 37, 40). Inset shows the best fit reference line for data of sample 8c.

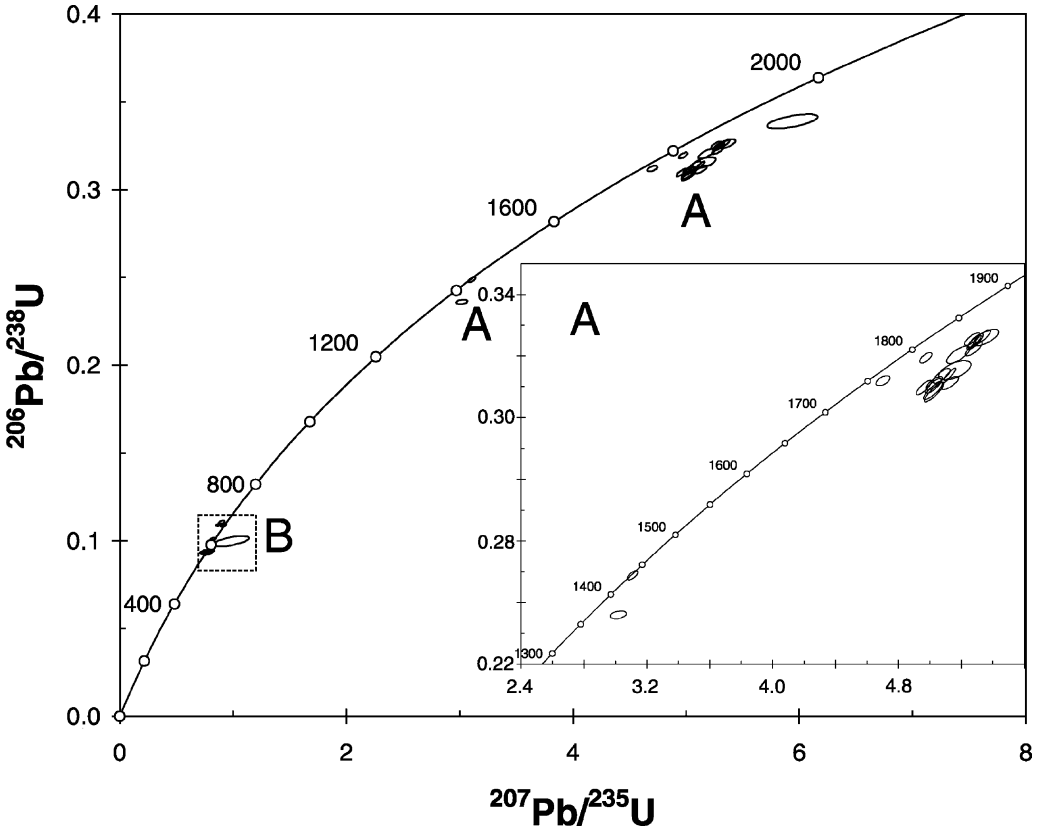

Fig. 5. Synoptic concordia diagram showing single grain U–Pb data of detrital zircons in all analysed Upper Vendian samples (18/19, 29). (A) Data of rounded detrital zircons (group I). (B) Data of euhedral detrital zircon (group IIa). Box around group IIa zircons indicates the area of uncertainty derived from initial lead correction using the maximum variation of $^{206}Pb/^{204}Pb$ and $^{207}Pb/^{204}Pb$ signatures in alkaline magmas (Wilson, 1996).

each sample population instead of having an overall uniform random scatter (Fig. 4). Thus, the zircon grains from the four samples appear to represent local age information related to the individual geological history of the original host rocks. All four clusters have elongate shapes oriented in an “en echelon” pattern subparallel to each other. However, they do not define distinct discordias.

5.2. Sample 8c

The population of six grains in this sample includes only those of group II (edge rounded prismatic grains). After correction for blank Pb and initial lead the $^{207}Pb/^{206}Pb$ apparent ages range from 1523 to 1859 Ma (Table 1). Assuming a young Pb loss event these apparent ages represent minimum ages for the crystallisation of the zircon. If older or several such events occurred, the age of crystallisation would definitely be higher.

Compared to the shapes of clusters of the other Riphean zircon populations (Fig. 4) that of sample 8c zircon rather resembles a discordia-like alignment of U–Pb-data. Under the presumption that the zircon grains have similar primary ages of crystallisation they must have suffered similar processes leading to discordancy. This concurs with the fact that all grains represent edge rounded euhedral zircon from S-type granites (group II; see above) indicating a similar source and less transport than group I zircons.

The upper intercept of the best fit reference line shows a value around 2006 Ma. This illustrates the

possible range of crystallization ages of granitic magmas in the source area. Yet due to the given pattern it is too speculative to give a reasonable interpretation for the lower intercept near the presumable age of sedimentation of the enclosing sandstone.

5.3. Sample 32

Twelve grains only of group I type were analysed from sample 32 (Fig. 4) showing a narrow range of $^{207}Pb/^{206}Pb$ apparent ages between 1958 and 2075 Ma (Table 1), but a wide scatter of U–Pb-data, because this population invariably contains rounded zircon fragments with multiple overprints, which is also reflected by the extremely low $^{206}Pb/^{204}Pb$ ratios. However, six more abraded grains show a much more reduced range of $^{207}Pb/^{206}Pb$ apparent ages between 1958 and 1989 Ma and a clustering near the concordia. This again is taken to point to an age of zircon crystallisation near 2000 Ma. Apparently improved results with more abraded zircons suggest strong influence by alteration subsequent to crystallisation regarding the strong discordancy of the other zircon grains in the population.

5.4. Samples 37 and 40

$^{207}Pb/^{206}Pb$ apparent ages of two grains (group I type) from sample 37 (Fig. 4) are the oldest (2124–2185 Ma) of the analysed Riphean zircon grains, those of six grains (groups I and II type) from sample 40 (Fig. 4) the youngest (1399–1572 Ma). The cluster of sample 40 shows that groups I and II zircons of its population have similar apparent ages suggesting similar histories. A derivation from a Riphean magmatic event, which might be suggested for sample 40 zircons with the lowest apparent $^{207}Pb/^{206}Pb$ ages, can be excluded on the basis of the observed zonation patterns and relatively low $^{206}Pb/^{204}Pb$ ratios. Such features point to a metamorphic origin of the zircons. A metamorphic event with $T > 150\,^{\circ}C$ between 1.8 and 0.65 Ma is not known yet for the Riphean sedimentary basin or for the source area for its sediments. Hence, the protolith ages of sample 40 zircons probably are in the same range as for the other Riphean samples.

The scatter of the U–Pb data in all four samples means that the U–Pb systems definitely experienced two or more effective geological processes. Internal features within the zircon grains suggest that the following effects could have led to discordancy:

(A) Effects in the source area: (1) magmatic growth on inherited cores as well as (2) metamorphic overgrowth and (3) annealing effects of strained lattices under high grade conditions.
(B) Effects of alteration in the sedimentary basin including diagenesis. All Riphean zircon crystals are more or less affected by alteration along cracks.

All age signatures are consistent with derivation from the pre-Riphean basement of the East European Platform (U–Pb age cluster of 1.8–2.3 Ga related to a Paleoproterozoic orogenic cycle; see above) representing high grade metamorphism and granite intrusion.

Two possibilities exist for the en echelon pattern of the U–Pb data of the Riphean samples:

1. Varying primary ages between 1.8 and 2.3 Ga, then at least two different events of lead loss (in the source area and the sedimentary basin).
2. Uniform primary ages, but variable lead loss after a first event followed by overprint during a second event.

Knowing that the zircon grains must have been affected by formation waters in the Riphean basin for at least the duration of the Upper Riphean one could assume a strong effect on lead loss. Such a mechanism would be rather likely in view of the fact that all Riphean zircon grains are at least slightly altered along cracks. Showing distinct U–Pb isotopic patterns for all samples the zircon crystals nevertheless reflect distinct events of lead loss as well as distinct source region signature.

5.5. Upper Vendian samples

The U–Pb systems of 31 Upper Vendian zircon crystals (samples 18/19, 29) were analysed (Fig. 5). Of these, four have $^{206}Pb/^{204}Pb$ ratios >500. These four all belong to the Vendian Group I zircon crystals. All Vendian Group II zircon crystals have remarkably low $^{206}Pb/^{204}Pb$ ratios (Table 1).

The four zircon crystals of *Vendian Group I type* which are characterized by higher amounts of radiogenic Pb have apparent $^{207}Pb/^{206}Pb$ ages of 1932,

1847, 1788 and 1483 Ma. Most other, but lower radiogenic Group I zircons (apparent $^{207}Pb/^{206}Pb$ ages 1898–2058 Ma, samples 18/19, 29) are within this range. Thus most of these data are certainly consistent with the assumption of a Paleoproterozoic origin of the Group I zircons. This is compatible with the presumed age of the Riphean detrital zircon and the major orogenic imprint in the East European Platform.

The zircons with lower apparent $^{207}Pb/^{206}Pb$ ages around 1439 and 1483 Ma (Fig. 5; sample 18/19) evidently did not suffer the same type or intensity of overprint as did the majority of the Vendian Group I zircons with higher apparent $^{207}Pb/^{206}Pb$ ages. These values might point to a later magmatic event within the Riphean basin. However, our data do not match with the 1350 Ma Mashak rift event in the Riphean basin presumed by Maslov et al. (1997; see Fig. 2). This would give further evidence for the allochthonous nature of the Beloretsk terrane, where the zircon grains are inferred to have been eroded.

Inspite of differences in zircon typologies the indication of a Paleoproterozoic origin suggests a common provenance from the eastern margin of the East European Platform for all Riphean and the Vendian Group I detrital zircons. This is also proved by the similarity of the Riphean and Upper Vendian heavy mineral spectrum (Willner et al., 2001).

Upper Vendian *Group IIa zircon crystals* (sample 18/19), which are classified as euhedral magmatic zircon without overprint and without rounding by their morphology and internal structures, were presumably delivered from one source, as can be assumed owing to their perfect pristine character and the coherence of zircon inclusions and detritus composition. The source can be identified as syenite as has been deduced above from mineral inclusions and the geological situation.

However, the content of radiogenic Pb and in consequence also the Pb-concentration are remarkably low in these zircon grains (Table 1). Apparent $^{207}Pb/^{206}Pb$ ages range from 643 to 512 Ma with a clustering of ages near the concordia around 580 Ma. However, in view of the low $^{206}Pb/^{204}Pb$ ratios the uncertainty of the isotope ratios used for the correction of the initial lead component becomes a crucial parameter for these data. We used the Stacey & Kramers model for common lead correction in Table 1. Using the maximum variation of $^{206}Pb/^{204}Pb$ and $^{207}Pb/^{204}Pb$ signatures in alkaline magmas (Wilson, 1996) which could also serve to derive the initial lead ratios in the zircons a larger range of uncertainty results (Fig. 5).

Despite the large errors resulting the U–Pb isotope data of the Vendian Group IIa zircon crystals do not contradict to age constraints given by Alekseev and Alekseeva (1980) and Glasmacher et al. (1999; see above) and with the presumed age of deposition of the Upper Riphean Kukkarauk-Formation (around 580 Ma, Maslov et al., 1997), from which the sandstone sample 18/19 was derived. The alkaline magmatic event would also be concomitant with the final exhumation of the Beloretsk terrane after 620 Ma.

6. Conclusions and implications for paleocontinental reconstructions

The following conclusions can be derived from the data presented:

- U–Pb-isotopic patterns as well as typological features of detrital zircon from Riphean and Upper Vendian sandstones are different. This gives further evidence for a change in detritus composition at around 620 Ma, when Upper Vendian sedimentation started.
- Clusters in the concordia diagram confined to single samples show remarkably strong influence of local sources on the composition of the detritus in spite of the large areas of discharge of detritus.
- Polycyclic rounded zircons with multiple overprint in the Riphean and Upper Vendian detritus show evidence of at least two events leading to lead loss. Alteration during diagenesis has been an important factor of lead loss.
- It can be confirmed that the age interval 1.8–2.3 Ga seems to be the significant age signature for the eastern margin of the Baltica protocontinent reflecting a major orogenic event. Both types of polycyclic zircon in the Riphean and Upper Vendian detritus first crystallized during this interval. Typological features show that they originally derived from high grade metamorphic rocks and granites.
- Zircon from the Upper Vendian detritus has two further sources apart from the majority of polycyclic zircon:
  - A few zircon grains with apparent $^{207}Pb/^{206}Pb$ ages around 1439 and 1483 Ma point to a later magmatic event, which is unknown in the

adjacent Riphean basin and underlines the allochthonous character of the source area.
- Euhedral zircons define a magmatic intrusion event of bimodal, partly alkaline magmas concomitant with the exhumation of the source area after 620 Ma.

The data match the Precambrian evolution in the Southern Urals as follows (Fig. 2):

Major constraints for the Neoproterozoic evolution of the Southern Urals are provided by Ar–Ar amphibole and white mica cooling ages between 720 and 540 Ma (Glasmacher et al., 1999, 2001) in the metamorphic complex of Beloretsk which contains high pressure rocks and is part of the supposed source area for the Upper Vendian detritus. Concomitant with this long history of exhumation, cooling, surface uplift, erosion and final emplacement of this complex bimodal, partly alkaline intrusions occurred that show no sign of overprint. During burial and early exhumation of the Beloretsk terrane, however, there was ongoing sedimentation in the Bashkirian basin further east. Upper Vendian foredeep sedimentation of detritus from the Beloretzk terrane started after 620 Ma and marks its final emplacement. Evidently the Beloretsk Terrane is an exotic continental block, but presumably also derived from Baltica as proved by the zircon age signatures in this study and by its heavy mineral spectra, which is similar to those of the Riphean sandstones (Willner et al., 2001).

A reasonable model explaining these major constraints would be a “Carribean-type” transpressional convergent margin setting. A good analog is the northern margin of South America that was originally a passive margin until the early Mesozoic and converted into a convergent one during displacement of high pressure rocks over a thousand km from the west along a major transcurrent fault system (Pindell and Barrett, 1990; Stöckhert et al., 1995). This also causes a major uplift within narrow high relief areas undergoing rapid erosion providing major detrital input into small foredeeps. Also alkaline magmatism is known from this setting (Lewis and Draper, 1990).

Many other features of a Neoproterozoic active continental margin have been detected along the entire length of the Urals and beyond represented by relics of the so-called Timanide orogen (Puchkov, 1997). These include HP/LT-rocks (Kvarkush Anticline of the Middle Urals, Puchkov, 1989), ophiolites (in the Polar Urals, Puchkov, 1997, Scarrow et al., 2001) and calc-alkaline magmatism (in the Polar Urals, Scarrow et al., 2001).

Prior to the existence of this Timanide active margin, the Riphean basin must have been situated at a stable continental margin. Such a geodynamic environment is compatible with numerous current paleocontinental reconstructions of different approaches such as those by Torsvik et al. (1996), Weil et al. (1998) or Rainbird et al. (1998). During the existence of the Rodinia supercontinent and its break-up, i.e. in the time of 1100–700 Ma, the entire eastern margin of Baltica was a stable margin of that continent continuing along its length into Siberia and Amazonia.

Furthermore we concur with recent reconstructions of Nance and Murphy (1994), Weil et al. (1998), Torsvik et al. (1996) and particularly with the suggestion of Scarrow et al. (2001) that the active Timanide margin of Baltica was a lateral extension of the Cadomian arc, which represented a collage of terranes in front of the W-African and Amazonian protocontinents that were still connected with Baltica (Fig. 6). The change to active margin conditions in the Southern Urals occurred after the Lower Vendian glaciation and lasted until the end of the Precambrian, when Baltica and West Gondwana separated.

It must also be noted that a similar history of zircon formation was detected in the continuation of the margin along the presumably neighbouring continental fragments of Amazonia and the Cadomian terranes. This history is characterized by a pronounced gap between Paleo- and Neoproterozoic zircon-forming orogenic events: Da Silva et al. (2000) report 2.0–2.2 Ga zircon ages from high grade gneisses in Southern Brazil overprinted by a 590 Ma event, Von Hoegen et al. (1990) show >2050 and 545 Ma zircon ages in detritus of the Belgian Brabant Massif (part of the “East Avalonia” terrane), and Tichomirowa et al. (2001) provide a comprehensive collection of zircon ages from gneisses in the East German Erzgebirge (part of the “Armorica” terrane) including 540–700 Ma and 2.1–2.2 Ga zircon-forming events. Evidently, this long history of coherent continental margins is characterized by a lack of Mesoproterozoic, especially “Grenvillian” events and a change to active margin conditions after a remarkably long orogenic silence.

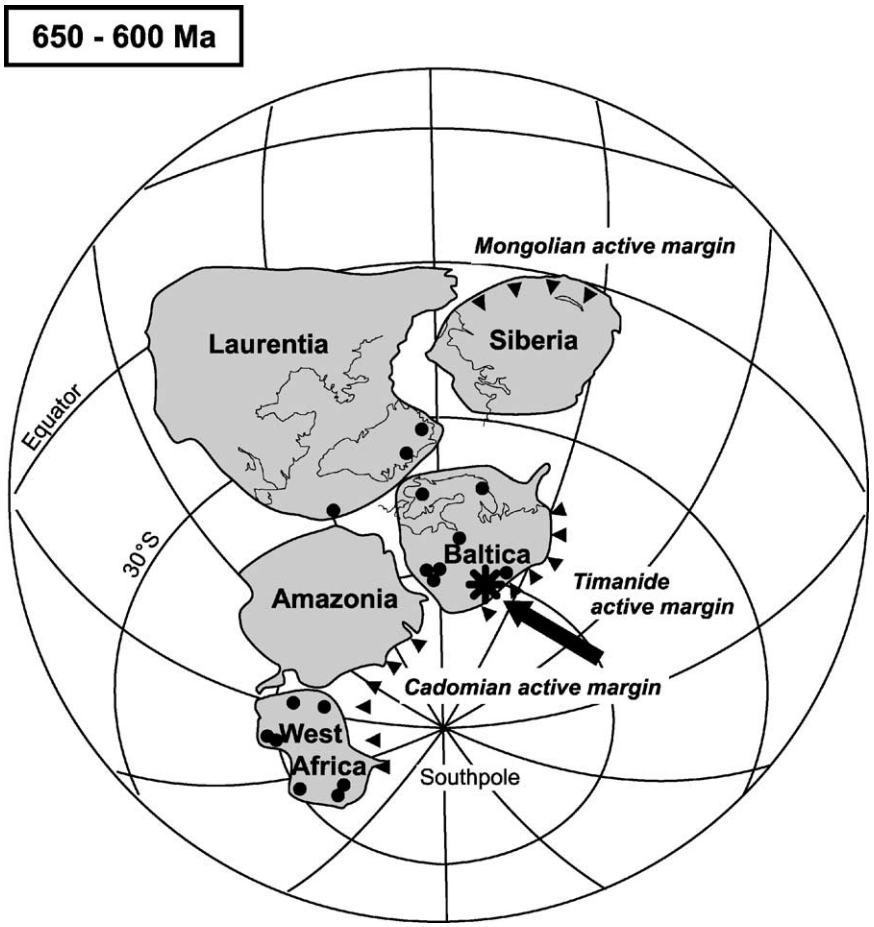

Fig. 6. Paleocontinental situation of the Southern Urals (asterisk/arrow) at the Eastern border of Baltica shortly after Lower Vendian glaciations (dots—glacial deposits). The reconstruction is of Torsvik et al. (1996) with the orientation of Siberia changed after Kravchinsky et al. (2001). The chain of active margins along this continental collage was formed between about 750 and 600 Ma and converted from a prior passive continental margin of the Rodinia supercontinent.

This is rather important, because Hartz and Torsvik (2002) recently questioned the mentioned reconstructions and alternatively place the eastern margin of Baltica opposite of Laurentia (E-Greenland) before 750 Ma. However, in this intracontinental position the Uralian Proterozoic detritus should show influence of the more variable East Laurentian age spectra as well, which predominantly contain 0.97–1.87 Ga age groups (Cawood and Nemchin, 2001; Watt and Thrane, 2001) including signatures of orogenic events in this period. There is neither an extension of the Riphean basin with continuous sedimentation from 1.63 to 0.65 Ga in Greenland nor any evidence of the 0.95 Ga orogen perpendicular to the Greenland continental margin (Watt and Thrane, 2001) in East Baltica.

After denudation of the Beloretsk Terrane during Cambrian, major extension occurred again (Puchkov, 1997) and from Ordovician until Late Devonian the western part of the Urals again became a stable continental margin along the entire eastern margin of Baltica.

Acknowledgements

Financial support by the Deutsche Forschungsgemeinschaft [grant Wi 875-6/1, 2] is gratefully

acknowledged. Perfect logistic support by the Ufa crew and invaluable field guidance by V.I. Kozlov and A.A. Alekseev during the 1999 field leg made this work possible. We also thank K. Mezger for providing facilities at the Laboratory of Geochronology at the University of Münster. Reviews particularly by P. Cawood and also by an anonymous referee substantially improved the paper. This paper is a contribution to EUROPROBE [URALIDES]. Europrobe is coordinated within the International Lithosphere Program and sponsored by the European Science Foundation. The paper is also a contribution to IGCP 440: Assembly and Breakup of Rodinia.

Appendix A. Petrographic characteristics of the samples

A.1. Riphean samples

Sample 8c (Upper Riphean Zilmerdak Formation) is a red laminated feldspathic sandstone with mm-thick laminae containing heavy mineral concentrations (mainly magnetite, ilmenite and zircon, but also tourmaline and rutile). Light minerals in the sandstone are composed of well rounded grains of predominantly monocrystalline quartz, both feldspars, white mica and abundant lithic clasts (chert, siltstone, acidic tuff). Quartz is the cement mineral.

Sample 32 (Upper Riphean Zilmerdak Formation) is a white, fine-grained, pure quartz arenite with primary well rounded quartz grains still detectable by minute inclusions along the original grain boundary against the quartzose matrix overgrown with optical continuity. Monocrystalline quartz clasts with abundant fluid inclusion trails are predominant, while perfectly round heavy minerals (tourmaline, rutile, zircon) and lithic fragments (quartz mylonite, chert, acidic tuff) occur as accessories.

Sample 37 (Middle Riphean Avzyan Formation) is a fine grained quartz arenite. The rock is well sorted and has a homogeneous grain size. Grains are moderately to well rounded with prominent quartz overgrowth. Undulous monocrystalline quartz is dominant. Plagioclase and K-feldspar is observed as well as few white mica, chlorite, opaques and tourmaline.

Sample 40 (Uppermost Riphean Krivoluk Formation) is a white quartz arenite, which shows similar characteristics as sample 32.

A.2. Upper Vendian samples

Sample 18/19 (Upper Vendian Kukkarauk Formation) is a coarse grained red quartzose sandstone. The sandstone contains mainly subrounded to rounded mono- and polycrystalline quartz, quartz mylonites, red chert, some quartz phyllite and rhyolite clasts. The heavy mineral spectrum is strongly reduced to about 80% zircon and some tourmaline and rutile. Conglomerates from the same locality contain abundant pebbles of quartz sandstone and quartz vein material, but also of abundant syenite and some rhyolite that are missing at other localities suggesting a rather local nearby source.

Four *samples* (*22, 23, 28, 29*; Upper Vendian Basa Formation) were investigated as one sample group (29), because rocks are petrographically identical, from the same sedimentary environment and were collected in close proximity of about 100 m along road outcrops. Furthermore, zircon is relatively rare in these horizons and hence, some concentration is necessary. All four samples are greenish medium grained litharenites from monotonous proximal grain flow deposits. They contain abundant angular to subangular, mono- and polycrystalline quartz and some feldspar clasts, detrital white mica and chlorite. Lithoclasts contain siliciclastic sedimentary material and low-grade metamorphic clasts in similar abundance. Acid and basic volcanic material is relatively rare. The heavy mineral spectrum is dominated by about 70% epidote, 5% apatite, 10% tourmaline, 10% rutile and only 5% zircon.

References

Alekseev, A.A., Alekseeva, G., 1980. Vendian alkaligabbros and their potassic suite in the SW Urals. Doklady Akad. Nauk USSR 255, 954–957 (in Russian).

Bogdanova, S.V., 1986. The Earth crust of the Russian platform in the Early Precambrian. Acad. Sci. USSR (Nauka) Moskow, 219 p. (in Russian).

Cawood, P.A., Nemchin, A.A., 2001. Paleogeographic development of the east Laurentian margin: constraints from U–Pb dating of detrital zircons in the Newfoundland Appalachians. Geol. Soc. Amer. Bull. 113, 1234–1246.

Da Silva, L.C., Hartmann, L.A., Mc Naughton, N.J., Fletcher, I., 2000. Zircon U–Pb SHRIMP dating of a Neoproterozoic overprint in Paleoproterozoic granitic-gneissic terranes, Southern Brazil. Am. Mineral. 85, 649–667.

Glasmacher, U.A., Reynolds, P., Alekseev, A.A., Puchkov, V.N., Taylor, K., Gorozhanin, V., Walter, R., 1999. $^{40}Ar/^{39}Ar$ thermochronology west of the Main Uralian fault, southern Urals, Russia. Geol. Rundsch. 87, 515–525.

Glasmacher, U.A., Bauer, W., Giese, U., Reynolds, P., Kober, B., Puchkov, V., Stroink, L., Alekseev, A.A., Willner, A.P., 2001. The metamorphic complex of Beloretzk, SW Urals, Russia—a terrane with a polyphase Meso- to Neoproterozoic tectonothermal evolution. Precambrian Res. 110, 185–213.

Ivanov, S.N., Krasnobaev, A.A., Rusin, A.I., 1986. Geodynamic regimes in the Precambrian of the Urals. Precambrian Res. 33, 189–208.

Jaffey, A.H., Flynn, K.F., Glendenin, L.E., Bentley, W.C., Essling, A.M., 1971. Precision measurement of half lives and specific activities of ^{235}U and ^{238}U. Phys. Rev. Sec. C Nucl. Phys. 4, 1889–1906.

Hartz, E.H., Torsvik, T.H., 2002. Baltica upside down: a new plate tectonic model for Rodinia and the Iapetus Ocean. Geology 30, 255–258.

Keller, B.M., Krasnobaev, A.A., 1983. Late Precambrian geochronology of the European part of the USSR. Geol. Mag. 120, 381–389.

Krasnobaev, A.A., 1986. Zircon as indicator of geological processes. Acad. Sci. USSR (Nauka) Moskow 145 p. [in Russian].

Kravchinsky, V.A., Konstantinov, K.M., Cogné, J.P., 2001. Paleomagnetic study of Vendian and Early Cambrian rocks of South Siberia and Central Mongolia: was the Siberian platform assembled at this time? Precambrian Res. 110, 61–92.

Kurz, S., 2000. Alterationsprozesse in Zirkon—Isotopen-geologische und geochemische Implikationen. Doctoral thesis Univ. Göttingen/Germany [unpublished], 112 p.

Lee, J.K.W., Tromp, J., 1995. Self-induced fracture generation in zircon. J. Geophys. Res. 100/B9, 17753–17770.

Lennykh, W.I. , Krasnobaev, A.A., 1978. Absolute ages of metamorphic rocks. In: Petrology and iron ore deposits of the Taratash Complex. Acad. Sci. USSR Sverdlovsk, pp. 69–76 [in Russian]

Lewis, J.F., Draper, G., 1990. Geology and tectonic evolution, northern Caribbean margin. In: Dengo, G., Case, J.E. (Eds.), The Caribbean region—vol. H, The Geology of North America. Boulder, Geological Society of America, pp. 77–140.

Maslov, A.V., Erdtmann, B.D., Ivanov, K.S., Krupenin, M.T., 1997. The main tectonic events, depositional history and the paleogeography of the southern Urals during the Riphean-early Palezoic. Tectonophysics 276, 313–335.

Medenbach, O., 1976. Geochemie der Elemente in Zirkon und ihre räumliche Verteilung.-Eine Untersuchung mit der EMS. doctoral thesis, Univ. Heidelberg/Germany, 58 p. [unpublished].

Nance, R.D., Murphy, J.B., 1994. Contrasting basement isotopic signatures and the palinspastic restoration of peripheral orogens: example from the Neoproterozoic Avalonian-Cadomian belt. Geology 22, 617–620.

Pindell, J.L., Barrett, S.F., 1990. Geological evolution of the Caribbean region; a plate-tectonic perspective. In: Dengo, G., Case, J.E. (Eds.), The Caribbean Region—vol. H. The Geology of North America, Boulder, Geological Society of America. pp. 405–432.

Puchkov, V.N., 1989. The collisional origin of the eclogite-glaucophane-schist belt of the Urals. Ofioliti 14, 213–220.

Puchkov, V.N., 1997. Structure and geodynamics of the Uralian orogen. In: Burg, J.-P., Ford, M. (Eds.), Orogeny Through Time. Geol. Soc. Am. Spec. Publ. 121, 201–236.

Pupin, J.P., 1980. Zircon and granite petrology. Contrib. Mineral Petrol. 73, 207–220.

Rainbird, R.H., Stern, R.A., Khudoley, A.K., Kropachev, A.P., Heaman, L.M., Sukhorukov, V.I., 1998. U–Pb geochronology of Riphean sandstone and gabbro from southeast Siberia and ist bearing on the Laurentia-Siberia connection. Earth Planet. Sci. Lett. 164, 409–420.

Scarrow, J.H., Pease, V., Fleutelot, C., Dushin, V., 2001. The late Neoproterozoic Enganepe ophiolite, Polar Urals, Russia: an extension of the Cadomian arc? Precambrian Res. 110, 255–275.

Schaltegger, U., Fanning, C.M., Günther, D., Maurin, J.C., Schulmann, K., Gebauer, D., 1999. Growth, annealing and recrystallisation of zircon and preservation of monazite in high-grade metamorphism: conventional and in-situ U–Pb isotope, cathodoluminescence and microchemical evidence. Contrib. Mineral. Petrol. 134, 186–201.

Sindern, S., Schulte, B., Kramm, U., 2001. Die tektonometamorphe Entwicklung des Taratash-Komplexes Mittlerer Ural Rußland. Eur. J. Min. 13 (Beiheft 1), 174.

Stacey, J.S., Kramers, J.D., 1975. Approximation of terrestrial lead isotope evolution by a two stage model. Earth. Planet. Sci. Lett. 6, 15–25.

Stöckhert, B., Maresch, W.V., Brix, M., Kaiser, C., Toetz, A., Kluge, R., Krückhans-Lueder, G., 1995. Crustal history of Margarita Island (Venezuela) in detail: constraint on the Carribean plate-tectonic scenario. Geology 23, 787–790.

Tichomirowa, M., Berger, H.J., Koch, E.A., Belyatski, B.V., Götze, J., Kempe, U., Nasdala, L., Schaltegger, U., 2001. Zircon ages of high-grade gneisses in the Eastern Erzgebirge (Central European Variscides)—constraints on the origin of the rocks and Precambrian to Ordovician magmatic events in the Variscan fold belt. Lithos 56, 303–332.

Torsvik, T.H., Smethurst, M.A., Meert, J.G., Van der Voo, R., McKerrow, W.S., Brasier, M.D., Sturt, B.A., Walderhaug, H.J., 1996. Continental break-up and collision in the Neoproterozoic and Paleozoic—a tale of Baltica and Laurentia. Earth Sci. Rev. 40, 229–258.

Vavra, G., Gebauer, D., Schmid, R., Compston, W., 1996. Multiple zircon growth and recrytallisation during polyphase Late Carboniferous to Triassic metamorphism in granulites of the Ivrea Zone (Southern Alps): an ion microprobe (SHRIMP) study. Contrib. Mineral. Petrol. 122, 337–358.

Vavra, G., Schmid, R., Gebauer, D., 1999. Internal morphology, habit and U–Th-Pb microanalysis of amphibolite-to-granulite facies zircons: geochronology of the Ivrea Zone (Southern Alps). Contrib. Mineral. Petrol. 134, 380–404.

Von Hoegen, J., Kramm, U., Walter, R., 1990. The Brabant Massif as part of Armorica/Gondwana: U–Pb isotopic evidence from detrital zircons. Tectonophysics 185, 37–50.

Watt, G.R., Thrane, K., 2001. Early Neoproterozoic events in East Greenland. Precambrian Res. 110, 165–184.

Weil, A.B., Van der Voo, R., Niocaill, C.M., Meert, J.G., 1998. The Proterozoic supercontinent Rodinia: paleomagnetically derived reconstructions for 1100–800 Ma. Earth Planet. Sci. Lett. 154, 13–24.

Wendt, J.I., 1993. Early Archean crustal evolution in Swaziland, southern Africa, as revealed by combined use of zircon geochronology, Pb–Pb and Sm-Nd systematics. Unpublished doctoral thesis, Univ. Mainz, Germany, 123 S.

Willner, A.P., Ermolaeva, T., Stroink, L., Glasmacher, U.A., Giese, U., Puchkov, V.N., Kozlov, V.I., Walter, R., 2001. Contrasting provenance signals in Riphean and Vendian sandstones in the SW Urals (Russia): constraints for a change from passive to active continental margin conditions in the Late Precambrian. Precambrian Res. 110, 185–213.

Wilson, M., 1996. Igneous Petrogenesis. Chapman & Hall, London, 466 p.